Article

Not peer-reviewed version

# Evaluation of the Activity of Amino Chalcone Against *Staphylococcus* Strains Harboring Efflux Pumps

Isydório Alves Donato , Cristina Rodrigues dos Santos Barbosa , Antonio Henrique Bezerra , Suieny Rodrigues Bezerra , Ray Silva Almeida , Cícera Datiane de Morais Oliveira Tintino , Isaac Moura Araújo , Ewerton Yago de Sousa Rodrigues , Maria Yasmin Cândido de Oliveira , Francisco Ferdinando Cajazeiras , Jayza Maria Lima Dias , Jesyka Macedo Guedes , Jéssica Híade Silva Cristino , Emmanuel Silva Marinho , Márcia Machado Marinho , Hélcio Silva dos Santos , Henrique Douglas Melo Coutinho , Saulo Relison Tintino * , Irwin Rose Alencar de Menezes * , Francisco Assis Bezerra da Cunha *

Posted Date: 25 September 2025

doi: 10.20944/preprints202509.2110.v1

Keywords: *Staphylococcus aureus*; chalcone; bacterial resistance; efflux pump; docking; ADMET; SYTOX

 doi:10.20944/preprints202509.2110.v1



*Article*

# Evaluation of the Activity of Amino Chalcone Against *Staphylococcus* Strains Harboring Efflux Pumps

**Isydório Alves Donato [1], Cristina Rodrigues dos Santos Barbosa [1], Antonio Henrique Bezerra [1], Suieny Rodrigues Bezerra [1], Ray Silva Almeida [2], Cícera Datiane de Morais Oliveira Tintino [2], Isaac Moura Araújo [2], Ewerton Yago de Sousa Rodrigues [1], Maria Yasmin Cândido de Oliveira [1], Francisco Ferdinando Cajazeiras [3], Jayza Maria Lima Dias [3], Jesyka Macedo Guedes [3], Jéssica Híade Silva Cristino [4], Emmanuel Silva Marinho [4], Márcia Machado Marinho [4], Hélcio Silva dos Santos [3], Henrique Douglas Melo Coutinho [2], Saulo Relison Tintino [1,*], Irwin Rose Alencar de Menezes [3*] and Francisco Assis Bezerra da Cunha [1,*]**

[1] Laboratory of Semiarid Bioprospecting (LABSEMA), Regional University of Cariri (URCA), Crato, CE, Brazil

[2] Laboratory of Microbiology and Molecular Biology, Department of Chemical Biology, Regional University of Cariri (URCA), Crato, CE, Brazil

[3] Chemistry Program, Vale do Acaraú State University (UVA), Sobral, CE, Brazil

[4] Graduate Program in Natural Sciences, State University of Ceará (UECE), Fortaleza, CE, Brazil

[5] Brazil National Institute of Science and Technology of the Health Economic–Industrial Complex (iCEIS); Laboratory of Phamacology and Chemical Molecular, Department of Chemical Biology, Regional University of Cariri (URCA), Crato, CE

* Correspondence: Irwin.alencar@urca.br (I.R.A.M.); cunha.urca@gmail.com (F.A.B.d.C.); Tel.: +55-88-98829724 (I.R.A.M.)

**Abstract**

The emergence of efflux-mediated resistance in *Staphylococcus aureus* has limited the effectiveness of conventional antibiotics, highlighting the need for novel adjuvant compounds. This study investigated the synthetic chalcone CMA4DMA as a potential modulator of bacterial resistance associated with the NorA efflux pump. In vitro antimicrobial assays showed that CMA4DMA displayed no intrinsic antibacterial effect (MIC ≥ 1024 μg/mL) but significantly reduced the minimum inhibitory concentration of norfloxacin and ethidium bromide in both wild-type SA1199 and NorA-overexpressing SA1199B strains. Fluorescence assays demonstrated increased intracellular accumulation of ethidium bromide without affecting membrane permeability, supporting an efflux-inhibitory mechanism. Molecular docking analysis revealed that CMA4DMA binds to the same site as norfloxacin in the NorA protein, engaging in hydrophobic and hydrogen-bond interactions with key residues, consistent with direct inhibition. In silico ADMET predictions indicated favorable oral absorption and distribution, though possible rapid metabolism and risks of hepatotoxicity and cardiotoxicity warrant caution for further development. Overall, CMA4DMA effectively restored antibiotic susceptibility in resistant *S. aureus* strains and showed a consistent inhibitory effect when compared with studies involving other efflux systems, reinforcing its potential as a promising scaffold for the development of new bacterial resistance modulators.

**Keywords:** *Staphylococcus aureus*; chalcone; bacterial resistance; efflux pump; docking; ADMET; SYTOX

## 1. Introduction

 doi:10.20944/preprints202509.2110.v1



The impact of antibiotic resistance on public health is severe and multifaceted. In addition to increasing infection-related mortality rates, it prolongs the course of diseases, raises treatment costs, and reduces social productivity. This phenomenon also undermines the effectiveness of various medical interventions, such as prophylactic surgeries and chemotherapy, which rely on the effective action of antibiotics to achieve success [1–3].

Among multidrug-resistant pathogens, several *Staphylococcus aureus* strains are particularly noteworthy. This microorganism poses a serious global health threat due to its high virulence, ability to evade the host immune system, and increasing resistance to antimicrobials [4–7].

Bacteria develop resistance to antibiotics through mechanisms such as genetic mutations, acquisition of resistance genes via horizontal gene transfer, and changes in gene expression. These adaptations can occur in both chromosomal DNA and mobile genetic elements, such as plasmids, which facilitate the rapid dissemination of resistance traits. Moreover, resistance can be mediated by strategies including enzymatic inactivation of the antibiotic, modification of the molecular target, activation of efflux pumps, and reduction of membrane permeability to drugs [8–10].

Among bacterial defense mechanisms against antibiotics, efflux pumps are of particular importance. These transmembrane proteins mediate drug extrusion, lowering their intracellular concentration and thereby enhancing microbial survival. Present in both Gram-positive and Gram-negative bacteria, efflux pumps represent promising targets for strategies aimed at restoring antibiotic efficacy. Inhibition of these proteins by specific compounds can reverse efflux-mediated resistance, enabling the reutilization of existing antimicrobials [11–14].

The NorA efflux pump, present in *Staphylococcus aureus*, belongs to the Major Facilitator Superfamily (MFS) and is composed of approximately 388 amino acids organized into 12 transmembrane domains that span the cytoplasmic membrane. Its primary function is the extrusion of toxic compounds, including several fluoroquinolones such as norfloxacin and ciprofloxacin, thereby reducing the intracellular concentration of these drugs and contributing to bacterial resistance [15]. The transport mechanism is a proton/drug antiport, utilizing the proton gradient to expel the substrate. NorA overexpression can be constitutive, as in the SA1199B strain, or induced upon exposure to antimicrobials. Due to its clinical relevance, NorA has been the focus of studies aiming to develop inhibitors capable of restoring antibiotic efficacy [16,17].

Chalcones have emerged as potential efflux pump inhibitors. These compounds, of natural or synthetic origin, have shown promising results in studies investigating their direct activity or synergistic effects with antibiotics, including the reduction of virulence factors such as biofilm formation and toxin production [18–22].

In this context, the present study aims to evaluate the potential of the chalcone CMA4DMA as an efflux pump inhibitor for use in combination with antibiotics against multidrug-resistant *Staphylococcus aureus* strains.

## 2. Results

### *2.1. In Vitro Antibacterial Activity*

#### 2.1.1. Evaluation of Minimum Inhibitory Concentration (MIC)

Upon analyzing direct antibacterial activity, it was observed that the chalcone exhibited no direct activity in the in vitro minimum inhibitory concentration (MIC) assay, with values equal to or greater than 1024 μg/mL for all strains, which is considered irrelevant for advancing to clinical studies. Regarding the standard efflux pump inhibitor CCCP, MIC values of 8 μg/mL for strain 1199 and 16 μg/mL for strain 1199B were identified. Bulleted lists look like this.

#### 2.1.2. Efflux Pump Inhibition by Modulation of Antibiotic and Ethidium Bromide MIC

In the analysis of potential MIC changes of antibiotics and ethidium bromide in the wild-type 1199 strain, it was observed that the chalcone was able to reduce the MIC of both the antibiotic and ethidium bromide. The antibiotic MIC decreased from 32 μg/mL to 8 μg/mL, and when the activity

 doi:10.20944/preprints202509.2110.v1



of ethidium bromide was evaluated in combination with the adjuvant, a similar reduction from 32 µg/mL to 8 µg/mL was observed. The positive control also reduced the MIC from 32 µg/mL to 0.5 µg/mL in both associations, as shown in Figure 1.

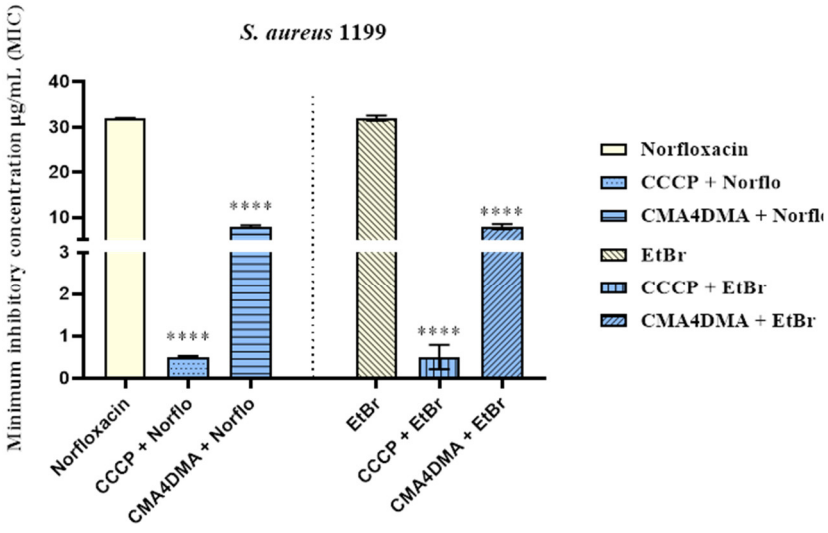


**Figure 1.** Evaluation of the ability to inhibit the NorA efflux pump by CMA4DMA against the S. aureus 1199 strain, in association with Norfloxacin and EtBr. Values represent the geometric mean ± SD (standard desviation). Analysis was performed using One-way ANOVA, followed by Tukey's test. **** = $p < 0.0001$ vs control.

Regarding the MIC changes in the NorA-overexpressing 1199B strain, it was observed that the chalcone, as an adjuvant, was able to reduce the MIC of both the antibiotic and ethidium bromide: from 64 µg/mL to 16 µg/mL for the antibiotic and from 64 µg/mL to 32 µg/mL for ethidium bromide. The positive control CCCP reduced the MIC from 64 µg/mL to 16 µg/mL for both the antibiotic and ethidium bromide, as shown in Figure 2.

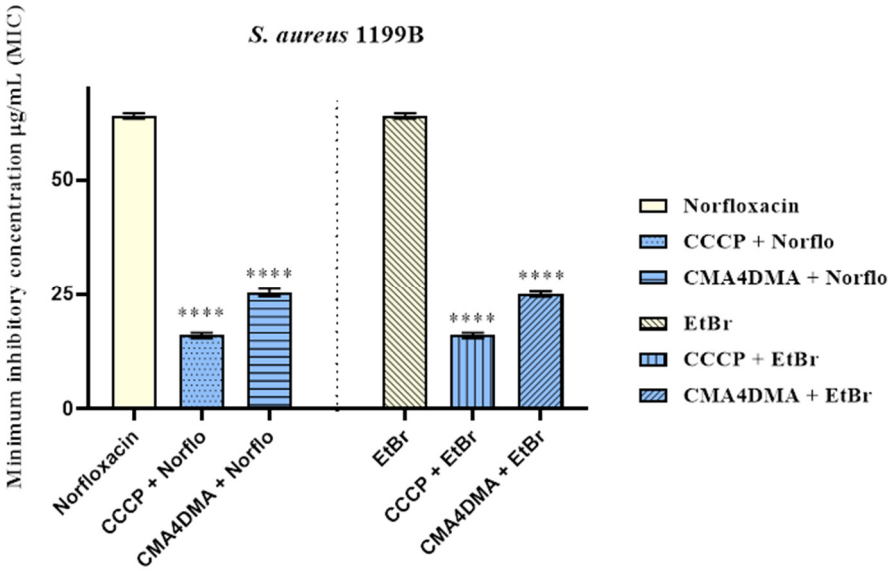


**Figure 2.** Evaluation of the ability to inhibit the NorA efflux pump by CMA4DMA against the S. aureus 1199B strain, in association with Norfloxacin and EtBr. Values represent the geometric mean ± SD (standard

 doi:10.20944/preprints202509.2110.v1



desviation). Analysis was performed using One-way ANOVA, followed by Tukey's test. **** = $p < 0.0001$ vs control.

### 2.1.3. Evaluation of NorA Efflux Pump Inhibition by Ethidium Bromide Fluorescence Measurement

In the assessment of ethidium bromide (EtBr) accumulation in S. aureus 1199B, CMA4DMA at 200 µg/mL caused a significant 15% increase in EtBr fluorescence compared to the negative control. A similar significant result was observed with the standard efflux pump inhibitor CCCP, which increased fluorescence by 21% in the 1199B strain (Figure 3).

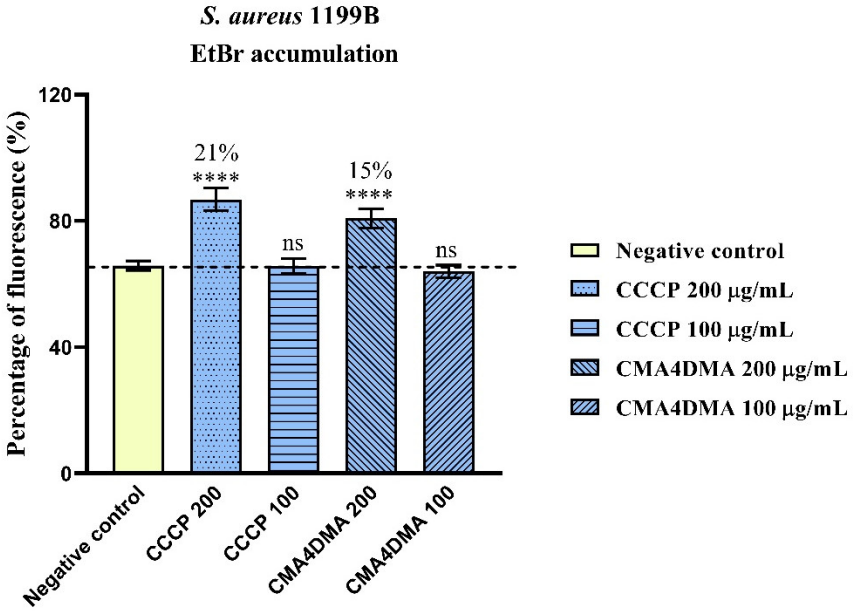


**Figure 3.** Evaluation of NorA efflux pump inhibition by CMA4DMA at 200 µg/mL and 100 µg/mL. Assessed by measuring EtBr fluorescence in S. aureus 1199B. Results are expressed as percentage of fluorescence. **** = $p < 0.0001$ vs negative control; ns = not significative.

### 2.1.4. Assessment of Increased Bacterial Membrane Permeability

It was observed that CMA4DMA at 200 µg/mL and 100 µg/mL did not increase SYTOX Green fluorescence intensity compared to the negative control in the tested strains, showing no statistically significant difference from the negative control. This indicates that the compound does not affect membrane permeability. The positive control, polymyxin B at 200 µg/mL and 100 µg/mL, significantly increased fluorescence intensity by 39% and 29% in S. aureus 1199B. Fluorescence measurements of SYTOX Green showed no statistically significant changes (Figure 4).

 doi:10.20944/preprints202509.2110.v1



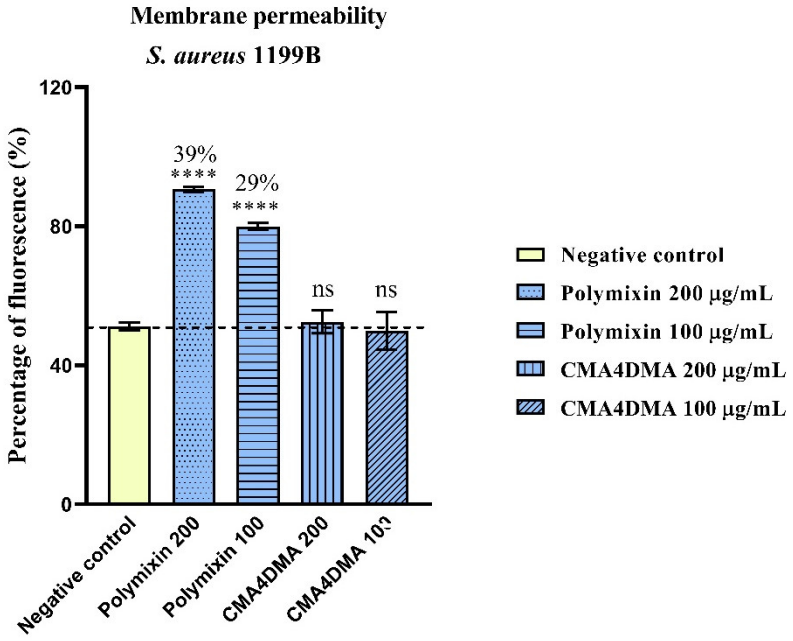


**Figure 4.** Evaluation of the action of CMA4DMA at 200 µg/mL and 100 µg/mL on the permeability of the bacterial membrane of S. aureus 1199B $p < 0.0001$ vs SYTOX Green. Results are expressed as mean fluorescence intensity.

*2.2. Molecular Docking Analysis*

When analyzing the docking simulation poses relative to the NorA efflux pump of *S. aureus* 1199B, it was observed that the chalcone CMA4DMA bound within the domain where the FAB antigen is complexed, occupying the same binding cavity as the antibiotics Norfloxacin and Ciprofloxacin, designated as the NorA efflux pump binding domain (Figure 5a). The cavity of this domain has a predicted molecular surface area of 1260.43 Å$^2$ (Figure 5b), where a greater spatial distance from the CCCP control can be noted, corroborating the experimental analyses, in which CCCP reduced the inhibitory concentration of Norfloxacin and EtBr. At the end of the cycle of 20 independent docking poses, CMA4DMA complexed with the NorA efflux pump with a binding affinity (BA) of –7.504 kcal/mol, which was energetically more favorable than Norfloxacin, which exhibited a BA of –7.242 kcal/mol (Table 1). All selected best-poses performed within a favorable statistical threshold of RMSD < 2.0 Å, ensuring reproducibility of the docking simulation protocol [25].

Analysis of ligand–receptor interactions revealed that CMA4DMA (green) formed hydrophobic interactions with the alkyl portions of residues Leu218, Ile309, Arg310, and Ile313, whereas Norfloxacin (blue) tended to form hydrophobic interactions with aromatic residues, including Phe140 and Phe303, which are neighboring residues within the binding domain cavity (Figure 5c) [23]. When compared with EtBr (Figure 5d), distinct interactions were observed, although near CMA4DMA, formed between the control and aromatic residues (Phe140, Tyr225, and Phe303). It is noteworthy that a hydrogen bond interaction was formed between the $NH_2$ group of CMA4DMA and the polar portion of Thr211, where the calculated donor–acceptor distance of 2.28 Å indicates moderate-to-weak polar interactions ($2.5 < d[Å] \leq 3.1$), with a stronger binding compared to Norfloxacin (d = 2.80 Å) [26].

 doi:10.20944/preprints202509.2110.v1



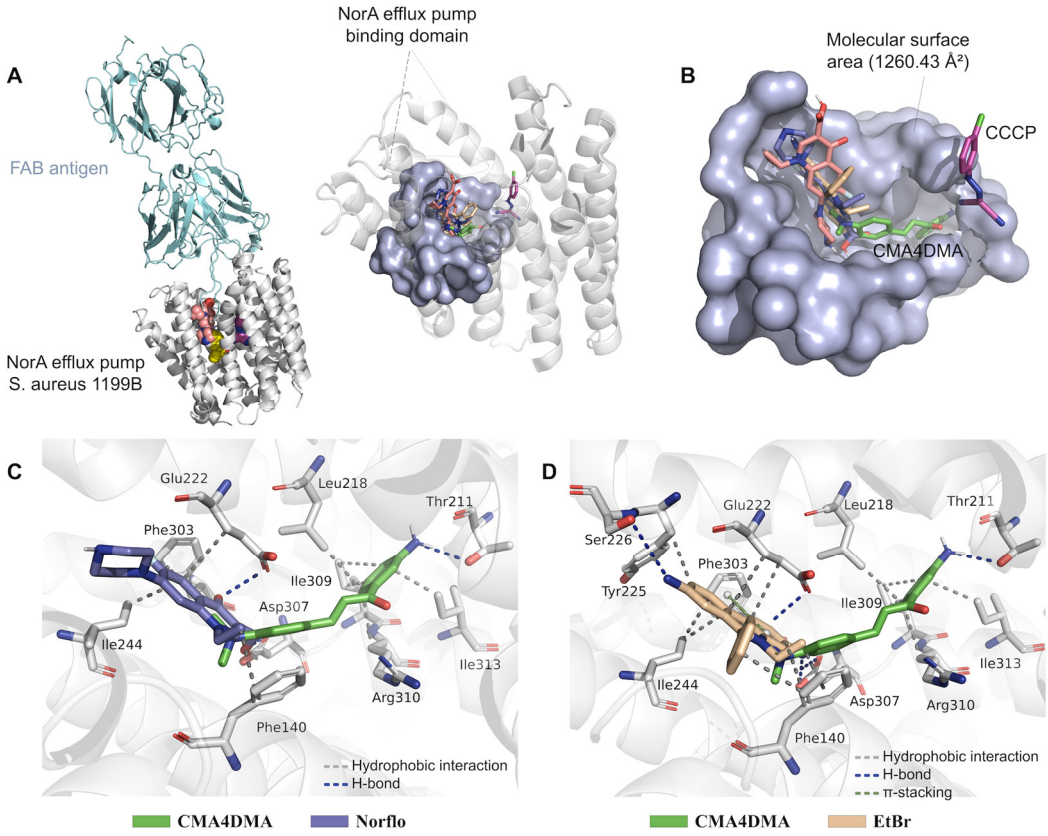


**Figure 5.** (A) Three-dimensional structure of the NorA efflux pump *S. aureus* 1199B (white) co-crystallized with the Fab antigen (cyan) and complexed with CMA4DMA chalcone, the antibiotics Norfloxacin and Ciprofloxacin, and EtBr and CCCP controls, highlighting the binding site (blue color). (B) Enlargement of the molecular surface area of the cavity predicted for the binding domain of the NorA efflux pump. (C) Three-dimensional visualization of the ligand-receptor interactions formed between the CMA4DMA ligands (green) and the antibiotic Norfloxacin (blue) and the residues of the binding domain of the NorA efflux pump. (D) Three-dimensional visualization of ligand-receptor interactions formed between CMA4DMA ligands (green) and EtBr control (orange) and residues of the NorA efflux pump binding domain.

**Table 1.** Data from ligand-receptor interactions observed in molecular docking simulations between chalcone CMA4DMA and control ligands (Norfloxacin, Ciprofloxacin, EtBr, and CCCP)* against NorA efflux pumps.

| Ligand | $E_A$ (kcal/mol) | RMSD (Å) | Ligand-receptor interactions | |
|---|---|---|---|---|
| | | | Type | Residue (distance in Å) |
| CMA4DMA | –7.504 | 0.118 | Hydrophobic | Leu218 (3.50), Ile309 (3.22), Ile309 (3.86), Arg310 (3.43), Ile313 (3.57) |
| | | | H-bond | Thr211 (2.28) |
| Norfloxacin* | –7.242 | 0.497 | Hydrophobic | Phe140 (3.61), Glu222 (3.94), Ile244 (3.60), Phe303 (3.51) |
| | | | H-bond | Glu222 (2.80), Asp307 (2.60) |
| Ciprofloxacin* | –6.427 | 1.748 | Hydrophobic | Glu222 (3.51), Ile240 (3.59), Ile244 (3.69), Ile244 (3.54) |
| | | | H-bond | Ser226 (2.77), Ser226(2.35), Asp307 (3.04) |
| EtBr* | –8.363 | 0.966 | Hydrophobic | Phe140 (3.81), Phe140 (3.59), Glu222 (3.88), Glu222 (3.88), |

 doi:10.20944/preprints202509.2110.v1



| | | | | |
|---|---|---|---|---|
| | | | | Tyr225 (3.58), Ile244 (3.64), Phe303 (3.69) |
| | | | H-bond | Ser226 (3.46), Asp307 (2.24) |
| | | | π-stacking | Phe303 (4.74) |
| CCCP* | –6.879 | 1.409 | Hydrophobic | Ile19 (3.83), Phe47 (3.97), Phe47 (3.65) |
| | | | H-bond | Gln51 (2.94), Asn340 (2.33) |

*2.3. In silico ADMET Study*

2.3.1. Cell Permeability Prediction

In the predictive ADMET analysis, effective cellular permeability (Papp) in Caco-2 cells showed a strong correlation with the calculated physicochemical parameters of lipophilicity (logP) and aqueous solubility (logS). For the predicted parameters, a statistical correlation of r = 0.93 was calculated, indicating a directly proportional relationship between Caco-2 Papp and logP. The compound CMA4DMA occupied a physicochemical space statistically closer to the controls EtBr and CCCP, where logPapp indices increased from –5.2 when logP exceeded 2.0 (Figure 6a). This indicates compounds with low affinity for aqueous environments (logS ≤ –3.0) and high cellular permeability.

In the *drug-like space radar* (Figure 6b), the calculated logP of 2.74 positioned CMA4DMA within the ideal lipophilicity range according to Pfizer's biopharmaceutical classification system (–2 < logP ≤ 5). Moreover, its molecular weight of 328.4 g/mol fell within the appropriate drug-like range (200–500 g/mol) (Table 2). The TPSA value of 46.33 Å$^2$, largely influenced by the $NH_2$ group, was within the optimal threshold for improving pharmacokinetic properties and reducing in vivo toxicity risk (40–90 Å$^2$). The QED score of 0.525 further supports the pharmacokinetic viability of the compound.

The predicted Papp value in Caco-2 cells was 1.38 × $10^{-5}$ cm/s, indicating higher intestinal permeability compared with Norfloxacin and Ciprofloxacin, which showed values below 1.0 × $10^{-5}$ cm/s (Table 3). In MDCK cells, predicted permeability values above 1.5 × $10^{-5}$ cm/s suggested that CMA4DMA, similarly to EtBr and CCCP, may present high permeability in more selective cell lines. The predicted probability of interaction with the efflux transporter P-gp indicated a low likelihood of CMA4DMA being a substrate, a characteristic associated with compounds of low polarity (TPSA ≤ 90 Å$^2$). Regarding distribution, the predicted Vdss of 0.37 L/kg suggested that the compound may distribute relatively evenly between blood plasma and biological tissues. Plasma protein binding predictions indicated PPB > 90%, likely due to the compound's low polarity and the hydrophobic nature of the molecule, favoring binding within the hydrophobic cavities of serum proteins.

**Table 2.** Physical-chemical properties calculated for CMA4DMA and applied to the quantitative estimation of druglikeness (QED) criterion[1].

| Property | Value | Optimal range |
|---|---|---|
| logP | 2.74 | ≤ 5.0 |
| logS | –3.78 | > –3.0 |
| MW (g/mol) | 266.14 | 200-500 |
| TPSA (Å$^2$) | 46.33 | 40-90 |
| nHA | 3 | ≤ 10 |
| nHD | 2 | ≤ 5 |
| nRot | 4 | ≤ 10 |
| AROM | 2 | ≤ 3 |
| QED[1] | 0.525 | - |

Note: QED was estimated from equation (1)[1].

 doi:10.20944/preprints202509.2110.v1



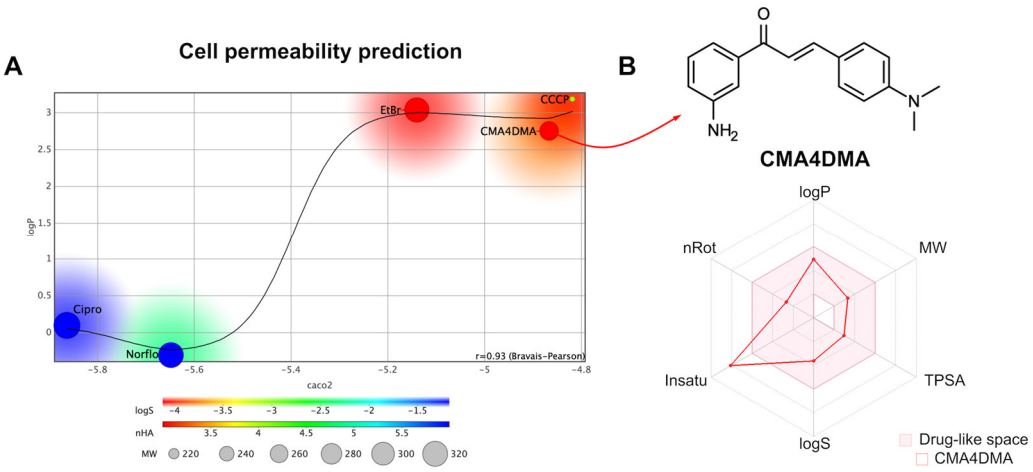


**Figure 6.** (A) Alignment between apparent permeability ($P_{app}$) in Caco-2 cells and logP and correlation with physicochemical descriptors of aqueous solubility (logS), molecular weight (MW), and number of H-bond acceptors (nHA), and (B) drug-like radar -like properties radar for the values calculated for CMA4DMA in relation to the thresholds of logP between –2.0-5.0, MW between 200-500 g/mol, TPSA between 20-120 Å$^2$, logS > –3.0, unsaturation (Fsp3 > 0.5) and nRot ≤ 10.

2.3.2. Brain and Intestinal Permeation and Cardiotoxicity

In the molecular lipophilicity potential (MLP) map, the structural contributions that favor human intestinal absorption (HIA) and blood–brain barrier (BBB) permeability were identified. Surface analysis indicated that the $NH_2$ group of CMA4DMA is highly polar and exhibits a large solvent-accessible surface area (red spectrum), whereas the substituted aromatic rings concentrate most of the compound's lipophilic surface (blue spectrum), resulting in a calculated logP of 2.74, consistent with optimal affinity for lipophilic environments (Figure 7a).

This property supports an estimated HIA of 88.76% (Figure 7b), as lipophilic compounds more readily permeate cell membranes and thus display enhanced absorption. The moderate-to-high lipophilicity (logP > 2.0–3.0) also favors permeability in selective cell lines, such as MDCK cells, commonly applied in BBB permeability assays. In this context, the predicted logBB of 0.87 correlated with the predicted MDCK permeability (Table 3), aligning with data observed for at least 87% of CNS-active compounds in the ADMET-LMC database (Figure 7c).

Additionally, the lipophilic nature of the substituted aromatic rings was associated with potential inhibition of hERG (human Ether-à-go-go-Related Gene) channels. In silico prediction suggested that the $\alpha,\beta$-unsaturated aromatic system contributes negatively to $K^+$-dependent hERG channel inhibition, yielding an estimated $IC_{50}$ of 6.104 µM and a $pIC_{50}$ of 5.21 ± 0.35 (Figure 7d). The data similarity test further predicted a potential inhibition pKi of 5.43 with 33% similarity to known hERG inhibitors (Figure 7e) and a predicted $pIC_{50}$ of 5.69 with 67% similarity to compounds documented as hERG inhibitors in the ADMET-LMC database (Figure 7f).

 doi:10.20944/preprints202509.2110.v1



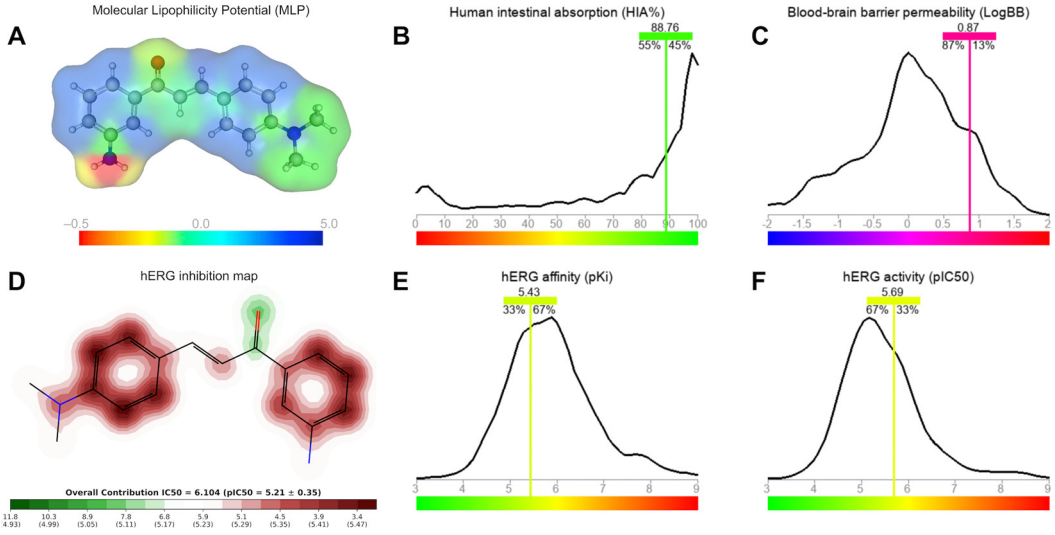


**Figure 7.** (A) Molecular lipophilicity potential (MLP) map, (B) human intestinal absorption (HIA) prediction, (C) Blood-brain barrier permeability (logBB) prediction, (D) 2D susceptibility map of inhibition of human Ether-a-go-go-Related Gene (hERG) K+-dependent channels, (E) hERG affinity expressed as inhibition potential (pKi), (F) hERG inhibition activity expressed as inhibitory concentration ($pIC_{50}$).

**Table 3.** Predicted pharmacokinetic properties of CMA4DMA through the multiplatform ADMET prediction approach.

| Property | CMA4DMA | Norflo | Cipro | EtBr | CCCP |
|---|---|---|---|---|---|
| $P_{app}$ Caco-2 (cm/s) | $1.38 \times 10^{-5}$ | $2.29 \times 10^{-6}$ | $1.38 \times 10^{-6}$ | $7.41 \times 10^{-6}$ | $1.54 \times 10^{-5}$ |
| $P_{app}$ MDCK (cm/s) | $1.90 \times 10^{-5}$ | $6.76 \times 10^{-6}$ | $6.02 \times 10^{-6}$ | $1.86 \times 10^{-5}$ | $1.55 \times 10^{-5}$ |
| P-gp (probability) | 0.04 | 0.99 | 0.98 | 0.99 | 0.00 |
| $CL_{Hepa}$ (µL/min/$10^6$ cells) | 76.50 | 12.81 | 2.90 | 55.67 | 64.28 |
| $CL_{Micro}$ (mL/min/kg) | 10.58 | 6.20 | 3.31 | 6.55 | 3.49 |
| $V_{dss}$ (L/kg) | 0.37 | 0.21 | 0.26 | 0.74 | –0.70 |
| PPB (%) | 94.31 | 20.36 | 25.51 | 83.13 | 97.99 |

2.3.3. Site of Metabolism and Rat Acute Toxicity

Prediction of the metabolic site indicated that CMA4DMA contains an $–N(CH_3)_2$ group, which contributes negatively (red color spectrum) to first-pass metabolism. This site was identified as an N-dealkylation site mediated by major CYP450 isoforms, including CYP2D6, CYP2C9, and CYP3A4 (Figure 8a). Such biotransformation may generate unstable aldehydes and free radicals capable of interacting with macromolecules such as DNA, potentially leading to hepatotoxic effects [38]. The data similarity test confirmed that this is a structurally specific metabolic site within acceptable similarity thresholds (Figure 8b) [39]. Predicted first-pass kinetics suggested a hepatic clearance (CLHepa) of 76.50 µL/min/$10^6$ cells, indicating that CMA4DMA could be more rapidly metabolized by hepatocytes than Norfloxacin and Ciprofloxacin, which exhibited CLHepa values below 15 µL/min/$10^6$ cells, consistent with greater metabolic stability and oral bioavailability (Table 3) [40].

 doi:10.20944/preprints202509.2110.v1



At the microsomal level, predicted clearance values (CLMicro) indicated that Norfloxacin and Ciprofloxacin are metabolically more stable (≤ 8.0 mL/min/kg) compared with CMA4DMA, which showed a predicted CLMicro of 10.58 mL/min/kg, reflecting relative metabolic instability and faster first-pass excretion of the chalcone (Table 3) [34]. Toxicity predictions in rats revealed an oral $LD_{50}$ of 1924 mg/kg, slightly below the general safety threshold ($LD_{50}$ > 2000 mg/kg), suggesting possible toxicity due to metabolic activation (Figure 8c) [41]. For parenteral routes, the predicted $LD_{50}$ values were < 500 mg/kg for intraperitoneal (IP) and intravenous (IV) administration, indicating greater systemic toxicity when first-pass metabolism is bypassed. For subcutaneous administration, the predicted $LD_{50}$ of approximately 893.7 mg/kg suggested that this route could be feasible, particularly for topical or localized infection therapies (Figure 8c).

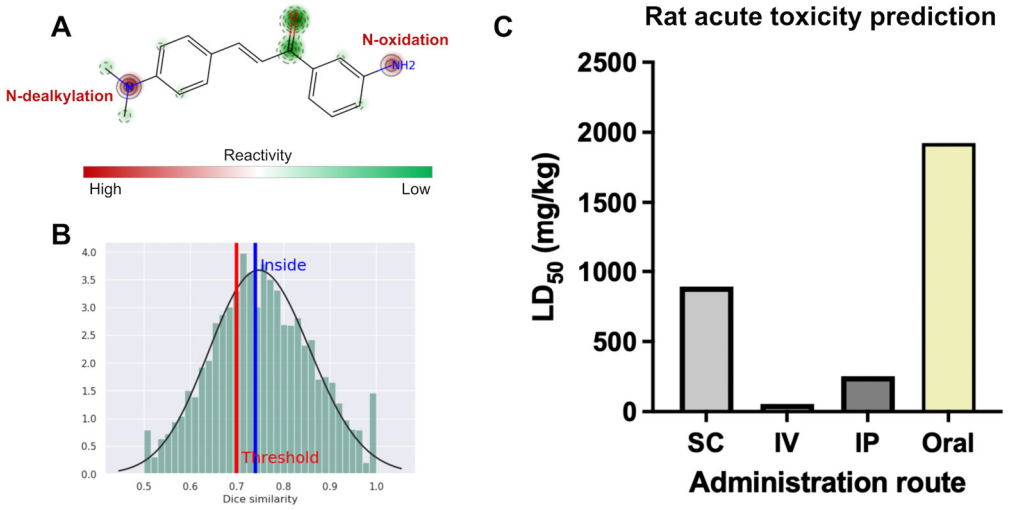


**Figure 8.** (A) 2D reactivity map and prediction of the metabolism site of the chalcone CMA4DMA, (B) similarity spectrum of data in relation to reactive fragments deposited in the STopTox training set, and (C) prediction of lethal dose ($LD_{50}$) in rats for different administration routes: oral, IP – intraperitoneal, IV – intravenous, and SC – subcutaneous.

## 3. Discussion

The lack of a relevant MIC does not entirely disqualify a substance for potential application in other studies against microorganisms, particularly when considering its possible use as an antibiotic adjuvant. In the case of efflux pump inhibitors, the absence of direct activity may even enhance their applicability, as previously noted in the literature [42].

Restoring the activity of antibiotics or other antibacterial agents through adjuvants is one of the main strategies currently employed to control strains harboring multiple mechanisms of resistance to antibacterial drugs or other bactericidal agents [43]. This is particularly relevant because the discovery of new effective antibiotics is increasingly rare. Furthermore, even when a new antibiotic is discovered, the likelihood that its indiscriminate use will lead to bacterial resistance is high [44]. Various methods exist to assess the ability of substances to restore antibiotic activity and, consequently, to identify the bacterial resistance mechanisms involved. Reduction of the minimum inhibitory concentration is one of the first analyses performed to indicate the restoration of antibiotic activity, typically using sub-inhibitory concentrations of the test substances in combination with an antibiotic or another antibacterial agent [45].

In the present study, as shown in Figure 1, CMA4DMA at sub-inhibitory concentrations was able to restore antibiotic activity by reducing the MIC, and the same effect was observed in combination with ethidium bromide. In the case of ethidium bromide, the MIC reduction is indicative

 doi:10.20944/preprints202509.2110.v1



of efflux pump inhibition, which is reinforced by the action of the positive control, the efflux pump inhibitor CCCP. It is also noteworthy that the SA1199 strain is a NorA efflux pump carrier with basal expression, and the observed MIC reduction in this strain may indicate inhibition of basal NorA pump expression, as illustrated in Figure 1 [46].

The SA1199B strain is widely described in the literature for its high resistance to norfloxacin and other quinolones [15,47]. Resistance to this class of antibiotics in *Staphylococcus aureus* can occur via efflux pumps or by modifications in topoisomerase, the primary target of quinolones [48]. MIC reduction in this strain, as observed in SA1199, may be associated with inhibition of previously described resistance mechanisms. The SA1199B strain overexpresses the NorA pump, and the decrease in MIC against certain antibiotics strongly suggests inhibition of this transporter, particularly when its expression is high in the bacterial cell membrane. To rule out interference from other mechanisms, it is common practice to evaluate MIC reduction of ethidium bromide, a characteristic substrate of NorA, alongside the effect of CCCP as a reference efflux pump inhibitor. Thus, the results presented in Figure 2 suggest that CMA4DMA has potential as a NorA pump inhibitor.

Studies with natural chalcones isolated from *Arrabidaea brachypoda* [49] and synthetic chalcones [18,50,51] have shown that, similarly to CMA4DMA, chalcones exhibit no direct antibacterial activity but significantly reduce the MIC of norfloxacin in SA1199B strains and of ethidium bromide, indicating NorA pump inhibition. Docking experiments confirmed ligand overlap with the norfloxacin binding site in NorA. These results are particularly similar to those observed with CMA4DMA, where the amino group on the phenolic ring contributed positively to MIC reduction in NorA-harboring strains [18,49,50].

In addition to the studies mentioned, the same chalcone used in the present work was investigated against *S. aureus* strains K4100, carrying QacC and β-lactamases [52], and K2068, carrying MepA [53]. No intrinsic activity (MIC ≥ 1024 μg/mL) was observed in either study. In the K4100 strain, CMA4DMA did not inhibit β-lactamase but significantly reduced the MIC of EtBr from 64 to 32 μg/mL. In the previously mentioned study against strain K2068, significant MIC reductions for ciprofloxacin and ethidium bromide were observed. Docking studies confirmed that the chalcone can bind to the same site occupied by the standard chlorpromazine inhibitor, interacting with key protein residues, which supports its potential as a MepA inhibitor, as it may have acted on NorA in the present study [52,53].

These studies complement and validate the results obtained in the present work, demonstrating that CMA4DMA consistently reduces efflux-mediated resistance in different *S. aureus* genetic backgrounds (NorA, MepA, and QacC), consolidating it as a promising antibacterial adjuvant candidate.

According to Figure 3, the increase in fluorescence due to greater intracellular ethidium bromide accumulation corroborates the MIC reduction results, supporting efflux pump inhibition. CMA4DMA was able to promote increased intracellular EtBr, making it more available to intercalate with bacterial DNA as a consequence of efflux pump inhibition, which normally extrudes the compound from the cell [54].

Therefore, according to Figure 4, the chalcone CMA4DMA did not alter membrane permeability, and thus its effect cannot be attributed to indirect efflux pump inhibition via changes in membrane fluidity. Although indirect inhibition through membrane alteration is one mode of action for compounds targeting efflux pumps, direct interaction with the pump is more common [55,56]. Exceptions exist, such as in the study by [57], where menadione was shown to act both directly on the efflux pump and indirectly on the plasma membrane, the latter also potentially disabling the pump. It is likely that CMA4DMA acts at a binding site on the NorA protein, as suggested by molecular docking studies.

Authors should discuss the results and how they can be interpreted from the perspective of previous studies and of the working hypotheses. The findings and their implications should be discussed in the broadest context possible. Future research directions may also be highlighted.

 doi:10.20944/preprints202509.2110.v1



The docking results indicate that CMA4DMA can effectively bind to the same NorA efflux pump domain where fluoroquinolone antibiotics such as Norfloxacin and Ciprofloxacin interact. The more favorable binding affinity of CMA4DMA compared to Norfloxacin suggests a higher energetic stability of this interaction, reinforcing its potential as a modulator of efflux activity.

The hydrophobic interactions of CMA4DMA with aliphatic residues (Leu218, Ile309, Arg310, and Ile313), distinct from the predominantly aromatic interactions observed for Norfloxacin and EtBr, reveal that CMA4DMA occupies the cavity in a differentiated binding mode. This divergence may favor synergistic effects with antibiotics, as the compound could alter the conformational dynamics of the binding pocket.

The hydrogen bonding observed between CMA4DMA and Thr211 further strengthens the binding profile, as the shorter donor–acceptor distance indicates more stable polar interactions compared to those of Norfloxacin. Importantly, the spatial distance of CMA4DMA relative to the CCCP control corroborates experimental findings, where CCCP potentiated the activity of Norfloxacin and EtBr, suggesting a mechanistic overlap in efflux pump inhibition.

Taken together, these findings support the hypothesis that CMA4DMA has a potential inhibitory effect on the NorA efflux pump, which may be potentiated in the presence of antibiotics. This interaction pattern highlights CMA4DMA as a promising candidate for further studies aimed at efflux pump modulation and antibiotic resistance reversal.

The predictive ADMET results indicate that CMA4DMA possesses physicochemical properties compatible with high cellular permeability, an attribute strongly correlated with lipophilicity (logP). Its placement in the *drug-like space radar*—within the thresholds of logP, MW, and TPSA—reinforces the compound's alignment with drug-like oral properties.

The predicted Papp value in Caco-2 cells, superior to that of the reference antibiotics Norfloxacin and Ciprofloxacin, suggests that CMA4DMA may exhibit higher intestinal absorption and, consequently, improved oral bioavailability. Additionally, the prediction of high permeability in MDCK cells and the low probability of being a P-gp substrate strengthen the perspective of efficient intracellular accumulation, favoring its antimicrobial potential.

The predicted Vdss, within the acceptable range, indicates that the compound may achieve a suitable balance between plasma and tissue distribution, minimizing the risk of excessive accumulation in specific compartments. The high level of plasma protein binding (>90%), although typical of low-polarity lipophilic molecules, may influence the free fraction available to exert pharmacological activity. Nonetheless, this feature may also contribute to plasma stability and prolonged circulation time. Overall, the ADMET analysis suggests that CMA4DMA combines favorable permeability, distribution, and pharmacokinetic viability, presenting advantages over comparative antibiotics in terms of absorption and cellular transport.

The MLP map and ADMET predictions suggest that the structural balance between polar and lipophilic regions in CMA4DMA is a key determinant of its pharmacokinetic profile. The predominance of lipophilic aromatic rings combined with a single polar $NH_2$ donor provides the compound with an optimal logP value of 2.74, which is associated with both high intestinal absorption and efficient membrane permeation. The predicted HIA of nearly 89% strongly supports the potential of CMA4DMA for oral administration, as lipophilicity is a critical determinant of absorption efficiency.

The predicted logBB and MDCK permeability values indicate that CMA4DMA may cross the BBB, displaying distribution patterns consistent with a large proportion of CNS-active compounds. While this property could support antimicrobial efficacy in tissues with selective barriers, it also raises concerns regarding potential off-target CNS effects.

A key safety consideration is the compound's predicted interaction with hERG channels. The $\alpha,\beta$-unsaturated aromatic system contributes to moderate hERG inhibition potential, with $IC_{50}$ and $pIC_{50}$ values suggesting partial blockade of $K^+$ channels. The data similarity to known hERG inhibitors (33–67%) highlights a moderate but significant risk for cardiotoxicity, particularly in scenarios of chronic exposure. These predictions emphasize the need for further experimental validation, as

 doi:10.20944/preprints202509.2110.v1



inhibition of hERG channels is strongly associated with arrhythmias and other cardiac disorders. Together, these findings indicate that CMA4DMA displays a favorable absorption and distribution profile, but its potential to interact with cardiac ion channels warrants caution and targeted safety evaluation.

The metabolic prediction highlights the $-N(CH_3)_2$ group of CMA4DMA as a major liability, acting as a specific site for N-dealkylation mediated by CYP450 isoforms. While this pathway contributes to clearance, it also poses a potential safety risk due to the possible generation of reactive intermediates such as aldehydes and free radicals, which could contribute to hepatotoxicity. This aligns with the observed moderate oral $LD_{50}$, which falls just below the threshold of non-toxic compounds, suggesting a risk of toxicity linked to metabolic activation.

Compared with Norfloxacin and Ciprofloxacin, CMA4DMA appears to be less metabolically stable, as reflected by its higher predicted hepatic and microsomal clearance values. This reduced metabolic stability implies lower oral bioavailability, as the compound would be more extensively metabolized during first-pass hepatic processing.

The predicted $LD_{50}$ values across different administration routes emphasize the role of first-pass metabolism in mitigating systemic toxicity. While oral administration may partially protect against systemic adverse effects, bypassing hepatic metabolism through intravenous or intraperitoneal administration results in greater predicted toxicity. Interestingly, the subcutaneous route showed an intermediate $LD_{50}$, suggesting potential viability for localized or topical applications, where systemic exposure could be minimized.

Taken together, these predictions suggest that although CMA4DMA has promising pharmacological attributes, its metabolic liability and associated toxicity risks require careful consideration. Optimization of structural features to reduce CYP-mediated N-dealkylation, or the exploration of alternative administration routes, may be essential for improving its therapeutic potential.

## 4. Materials and Methods

### *4.1. Chemical Synthesis*

The chalcone CMA4DMA was synthesized through a Claisen–Schmidt condensation reaction under basic conditions, using 3-aminoacetophenone and 4-(dimethylamino)benzaldehyde [52].

### *4.2. Molecular Docking of NorA and CMA4DMA*

For the theoretical investigation of the antimicrobial effect against *S. aureus*, the protein model of the NorA efflux pump from the 1199B strain was obtained from the RCSB Protein Data Bank repository (https://www.rcsb.org/), deposited under PDB ID 7LO7. This structure is classified as a transporter protein expressed in E. coli, with its three-dimensional conformation resolved by electron microscopy at a 3.74 Å resolution. For protein preparation prior to molecular docking simulations, AutoDockTools™ (https://autodocksuite.scripps.edu/adt/) was used to add hydrogen atoms, compute Gasteiger charges, and adjust the grid-box parameters. The grid-box was configured to cover the entire conformational space of the protein, with dimensions x = 54, y = 58, and z = 62, centered at x = 137.578, y = 138.065, and z = 156.646. Subsequently, AutoDock Vina™ (https://vina.scripps.edu/) was set to perform 50 independent simulations of 20 poses each, for all ligands optimized using the Merck Molecular Force Field method (MMFF94) in Avogadro 2 (https://two.avogadro.cc/). The ligands included CMA4DMA, the antibiotics norfloxacin and ciprofloxacin, and the controls EtBr and CCCP. The best pose selection criteria were based on binding affinity energy (EA) lower than –6.0 kcal/mol and Root Mean Square Deviation (RMSD) below 2.0 Å, as statistical validation parameters [58].

### *4.3. Molecular Docking of NorA and CMA4DMA*

 doi:10.20944/preprints202509.2110.v1



For the analysis of absorption, distribution, metabolism, excretion, and toxicity (ADMET) properties, a predictive protocol based on the quantitative estimate of drug-likeness (QED) was applied, as shown in Equation (1):

$$QED = exp\left(\frac{1}{n}\sum_{i=1}^{n} \quad lnd_i\right) \quad (1$$

where n is the number of physicochemical properties (i) calculated, and d is the desirability function, which considers the thresholds defined as follows: molecular weight (MW) ≤ 500 g/mol, lipophilicity (logP) ≤ 5, hydrogen bond donors (HBD) ≤ 5, hydrogen bond acceptors (HBA) ≤ 5, topological polar surface area (TPSA) ≤ 140 Å², rotatable bonds (nRot) ≤ 10, aromatic rings ≤ 3, and structural alerts ≤ 1 (n = 8). The summation yields a score ranging from 0.0 (poor drug-likeness) to 1.0 (optimal drug-likeness) [59]. The alignment of these descriptors was analyzed according to Lipinski's rules [60], the Pfizer rule [61], the Golden Triangle rule [27], and the GlaxoSmithKline (GSK) rule.

For the prediction of pharmacokinetic descriptors, the following servers were used: ADMETlab 3.0 (https://admetlab3.scbdd.com/), ADMET-AI (https://admet.ai.greenstonebio.com/), ADMET–LMC (http://qsar.chem.msu.ru/admet/), Pred-hERG (https://predherg.labmol.com.br/), and SwissADME (http://www.swissadme.ch/). The properties analyzed included effective cellular permeability (Papp), human intestinal absorption (HIA), blood–brain barrier (BBB) permeability, hepatic clearance (CLHepa), volume of distribution (Vdss), and cardiotoxicity via human Ether-à-go-go-Related Gene (hERG) inhibition.

For the prediction of metabolic sites, the servers SMARTCyp (https://smartcyp.sund.ku.dk/mol_to_som), FAME 3 (https://nerdd.univie.ac.at/fame3), and StopTox (https://stoptox.mml.unc.edu/) were employed. The analysis of fragments susceptible to cytochrome P450 (CYP450)-dependent metabolism was correlated with the prediction of lethal dose (LD50) in rats using the GUSAR Online server (https://www.way2drug.com/gusar/).

### *4.4. In Vitro Antibacterial Activity*

#### 4.4.1. Bacterial Strains

In this study, the *S. aureus* strains SA-1199 (wild-type) and SA-1199B were used. The SA-1199B strain overexpresses the NorA efflux protein, which is associated with resistance to fluoroquinolone-class substrates, such as norfloxacin.

The strains were kindly provided by Prof. S. Gibbons (University of London, Malet St, Bloomsbury, London WC1E 7HU, United Kingdom) and Prof. G. W. Kaatz (Wayne State University School of Medicine, Detroit, Michigan, USA) and maintained on blood agar (Difco Laboratories Ltd., São Paulo, Brazil). The strains are preserved by cryopreservation at –80°C in glycerol solution at the Laboratory of Microbiology and Molecular Biology, Regional University of Cariri (URCA). For experimental preparation, the strains were cultured for 24 hours at 37°C in brain–heart infusion agar (BHI Agar, Acumedia Manufacturers Inc.).

#### 4.4.2. Culture Media

The culture media used for the microbiological assays were as follows: Brain Heart Infusion Agar (BHI Agar, Acumedia Manufacturers Inc.), prepared according to the manufacturer's instructions, and Brain Heart Infusion (BHI, Acumedia Manufacturers Inc.) prepared at a 10% concentration.

#### 4.4.3. Substances

The antibiotics (norfloxacin and ciprofloxacin) and the chalcone CMA4DMA were dissolved in dimethyl sulfoxide (DMSO) and sterile water, with the DMSO proportion kept below 5%. Ethidium bromide (EtBr) was dissolved in sterile distilled water, while carbonyl cyanide m-chlorophenyl hydrazone (CCCP) was dissolved in methanol/water (1:1, v/v). All substances were prepared at a standard concentration of 1024 μg/mL.

 doi:10.20944/preprints202509.2110.v1



4.4.4. Determination of Minimum Inhibitory Concentration (MIC)

The MIC of the chalcone CMA4DMA was determined according to the broth microdilution method described by [62], with modifications. The strains used in the assays were cultured 24 hours prior to the experiments. After this period, the bacterial inoculum was suspended in saline solution corresponding to 0.5 McFarland standard, approximately 1.5 × $10^8$ CFU/mL. Subsequently, microtubes were filled with 900 µL of BHI and 100 µL of the inoculum, and the plates were loaded with 100 µL of the final solution. Microdilution was performed with 100 µL of CMA4DMA in serial dilutions up to the penultimate well of the plate (1:1), with the last well used as a growth control. Compound concentrations ranged from 512 µg/mL to 8.0 µg/mL. After 24 hours of incubation, readings were performed by adding 20 µL of resazurin (7-hydroxy-10-oxidophenoxazin-10-ium-3-one). Resazurin is oxidized in the presence of acidic medium caused by bacterial growth, inducing a color change from blue to pink [63]. The MIC was defined as the lowest concentration at which no visible growth was observed [64]. All assays were performed in triplicate.

4.4.5. Evaluation of Efflux Pump Inhibition by Modification of the Antibiotic and Ethidium Bromide MIC

To investigate whether the chalcone CMA4DMA acts as a potential NorA efflux pump inhibitor, a comparative study was conducted between the effects of standard pump inhibitors, evaluating their ability to reduce the MIC of EtBr and antibiotics. The standard inhibitor CCCP was used to validate NorA pump expression in the tested strain. Efflux pump inhibition was tested using sub-inhibitory concentrations (MIC/8) of both the inhibitors and the chalcone. In the assays, 150 µL of each bacterial inoculum, suspended in saline solution corresponding to 0.5 McFarland standard (approximately 1.5 × $10^8$ CFU/mL), was added together with the inhibitors and the chalcone (MIC/8) and completed with BHI. Subsequently, the mixtures were transferred to 96-well microdilution plates, to which 100 µL of antibiotic or EtBr in serial dilutions (1:1) ranging from 512 to 0.5 µg/mL were added. Plates were incubated at 37°C for 24 hours, and bacterial growth was assessed using resazurin (7-hydroxy-10-oxidophenoxazin-10-ium-3-one). Resazurin is oxidized in the presence of acidic medium resulting from bacterial growth, inducing a color change from blue to pink [63]. The MIC was defined as the lowest concentration at which no visible growth was observed [64]. MICs of the controls were determined using plates containing only antibiotics or EtBr. All tests were performed in triplicate.

4.4.6. NorA Efflux Pump Inhibitory Activity Assessed by Increased EtBr Fluorescence Emission

For this assay, the *S. aureus* 1199B strain expressing the NorA efflux pump was used. Strains were streaked on Mueller Hinton agar 24 hours prior to the experiment and maintained in a bacteriological incubator at 37°C. The inoculum was prepared in phosphate-buffered saline (PBS) to a 0.5 McFarland standard and distributed into black 96-well plates. In the test groups, CMA4DMA was added at final concentrations of 200 and 100 µg/mL. The negative control consisted of PBS prepared under the same dilution conditions as the test substance, followed by the addition of bacteria. The positive control consisted of CCCP at 200 µg/mL and 100 µg/mL. Plates were incubated for 1 hour, after which EtBr (2 µg/mL) was added to all wells. The plates were then incubated again and fluorescence was measured using a Cytation 1 microplate reader (BioTek®, Winooski, VT, USA) with Gen5™ 3.11 software. Excitation was set at 530 nm and emission at 590 nm [62].

4.4.7. Assessment of Bacterial Membrane Permeability Using SYTOX Green Fluorescence Assay

For this assay, the DNA-intercalating dye SYTOX Green was used. The bacterial inoculum of *S. aureus* 1199B was prepared and distributed into black 96-well plates. CMA4DMA was added at final concentrations of 200 and 100 µg/mL. Polymyxin B was used as a positive control at 200 and 100 µg/mL, while phosphate-buffered saline (PBS) served as the negative control. Plates were incubated for 1 hour. Subsequently, 100 µL of SYTOX Green at a final concentration of 1 µM was added. Plates were incubated for an additional hour, and fluorescence was measured using a Cytation 1 microplate

 doi:10.20944/preprints202509.2110.v1



reader (BioTek®, Winooski, VT, USA) with Gen5™ 3.11 software. Excitation and emission wavelengths were set at 485 nm and 528 nm, respectively. All assays were performed in triplicate [65].

4.4.8. Statistical Analysis

The results were analyzed using one-way ANOVA, followed by Tukey's post hoc test. Microbiological results for MIC reduction were expressed as geometric mean ± SD, while results from efflux pump inhibition mechanism assays were expressed as arithmetic mean ± SD. Values of $p < 0.05$ were considered statistically significant. GraphPad Prism 5.0 software was used for all analyses. All assays were performed in triplicate.

## 5. Conclusions

The in vitro assays demonstrated that the chalcone CMA4DMA, although devoid of direct antibacterial activity (MIC ≥ 1024 μg/mL), significantly enhanced the action of norfloxacin and ethidium bromide in *Staphylococcus aureus* strains carrying the NorA efflux pump. This potentiation was evidenced by reduced MIC values and increased intracellular EtBr fluorescence, without compromising bacterial membrane integrity. These experimental findings corroborate the in silico analyses, which revealed a strong interaction of CMA4DMA with the NorA binding site, supporting its role as a direct efflux pump inhibitor. Thus, the combination of computational and microbiological data reinforces the potential of CMA4DMA as an antimicrobial adjuvant to restore antibiotic efficacy against resistant strains, although additional studies on pharmacokinetics, toxicity, and preclinical models are required to confirm its therapeutic feasibility.

**Author Contributions:** Conceptualization, all authors.; methodology, all authors; formal analysis, I.A.D, S.R.T.; investigation, I.A.D, C.R.S.B, A.H.B, E.S.M.; resources, H.S.S, H.D.M.C, S.R.B, F.A.B.C.; data curation, I.A.D, C.D.M.O.T, A.H.B, S.R.B.; writing—original draft preparation, I.A.D, C.D.M.O.T, H.S.S, E.S.M.; writing—review and editing, I.A.D, S.R.T.; visualization, I.A.D, S.R.T.; supervision, I.R.A.M., S.R.T, F.A.B.C.; project administration, I.R.A.M., I.A.D, S.R.T and F.A.B.C.; funding acquisition, H.S.S, H.D.M.C, S.R.T. and F.A.B.C. All authors have read and agreed to the published version of the manuscript.

**Funding:** This study was financed in part by the Conselho Conselho Nacional de Desenvolvimento Científico e Tecnológico – Brasil -CNPq (to F.A.B.C.– process: 306008/2022-0, 303164/2022-0 and 405394/2023-3; I.R.A.M. process 303940/2022-0, 441128/2023-8, 404780/2021-0 and 303438/2021-5), Fundação Cearense de Apoio ao Desenvolvimento Científico e Tecnológico – FUNCAP UNIVERSAL (process: UNI-0210-00337.01.00/23), FUNCAP-INTERNACIONALIZAÇÃO (process: ITR-0214-00060.01.00/23), PDCTR (CNPq/FUNCAP) (process: DCT-0182-00048.02.00/21 and 04879791/2022) and FUNCAP (process: BP5-0197-00174.01.00/22 and FPD-0213-00369.01.00/23).

**Informed Consent Statement:** Informed consent was obtained from all subjects involved in the study.

**Data Availability Statement:** Data is available from the authors upon reasonable request.

**Acknowledgments:** The authors thank Fundação Cearense de Apoio ao Desenvolvimento Científico e Tecnológico (Funcap), Coordenação de Aperfeiçoamento de Pessoal de Nível Superior (CAPES) and Conselho Nacional de Desenvolvimento Científico e Tecnológico (CNPq) for financial support and scholarship. and the authors thank Northeastern Center for the Application and Use of Nuclear Magnetic Resonance (CENAUREMN), National Institute of Science and Technology of the Health Economic–Industrial Complex (iCEIS) for their financial support.

**Conflicts of Interest:** The authors declare no conflicts of interest.

## Abbreviations

The following abbreviations are used in this manuscript:

 doi:10.20944/preprints202509.2110.v1



| | |
|---|---|
| ADMET | Absorption, Distribution, Metabolism, Excretion, and Toxicity |
| CCCP | Carbonyl Cyanide M-Chlorophenyl Hydrazone |
| CMA4DMA | chalcone(2E)-1-(30-aminophenyl) 3-(4-dimethylaminophenyl)-prop-2-en-1-one |
| DMSO | Dimethyl Sulfoxide |
| DNA | Deoxyribonucleic Acid |
| DOAJ | Directory of open access journals |
| EA | Affinity Energy |
| EtBr | Ethidium Bromide |
| HBD | Hydrogen Bond Donor |
| HIA | Human Intestinal Absorption |
| LD | Linear dichroism |
| MDPI | Multidisciplinary Digital Publishing Institute |
| MFS | Major Facilitator Superfamily |
| MIC | Minimum Inhibitory Concentration |
| MLP | Molecular Lipophilicity Potential |
| MW | Molecular Weight |
| PBS | Phosphate-Buffered Saline |
| PPB | High Plasma Protein Binding |
| RMSD | Root Mean Square Deviation |
| TLA | Three letter acronym |
| TPSA | Topological Polar Surface Area |

## References


1. D. Chinemerem Nwobodo, M.C. Ugwu, C. Oliseloke Anie, M.T.S. Al-Ouqaili, J. Chinedu Ikem, U. Victor Chigozie, M. Saki, Antibiotic resistance: The challenges and some emerging strategies for tackling a global menace, J Clin Lab Anal 36 (2022). https://doi.org/10.1002/jcla.24655.
2. V. Lazar, E. Oprea, L.M. Ditu, Resistance, Tolerance, Virulence and Bacterial Pathogen Fitness—Current State and Envisioned Solutions for the Near Future, Pathogens 12 (2023). https://doi.org/10.3390/pathogens12050746.
3. H. Tahmasebi, N. Arjmand, M. Monemi, A. Babaeizad, F. Alibabaei, N. Alibabaei, A. Bahar, V. Oksenych, M. Eslami, From Cure to Crisis: Understanding the Evolution of Antibiotic-Resistant Bacteria in Human Microbiota, Biomolecules 15 (2025). https://doi.org/10.3390/biom15010093.
4. G. Cheung, J. Bae, M. Otto, Pathogenicity and virulence of *Staphylococcus aureus*, Virulence 12 (2021) 547–569. https://doi.org/10.1080/21505594.2021.1878688.
5. M. Gajdács, The Continuing Threat of Methicillin-Resistant *Staphylococcus aureus*, Antibiotics 8 (2019). https://doi.org/10.3390/antibiotics8020052.
6. A. Horswill, C. Jenul, Regulation of *Staphylococcus aureus* Virulence, Microbiol Spectr 7 (2019). https://doi.org/10.1128/microbiolspec.gpp3-0031-2018.
7. A. Horswill, J. Kwiecinski, *Staphylococcus aureus* bloodstream infections: pathogenesis and regulatory mechanisms., Curr Opin Microbiol 53 (2020) 51–60. https://doi.org/10.1016/j.mib.2020.02.005.
8. E.M. Darby, E. Trampari, P. Siasat, M.S. Gaya, I. Alav, M.A. Webber, J.M.A. Blair, Molecular mechanisms of antibiotic resistance revisited, Nat Rev Microbiol 21 (2023) 280–295. https://doi.org/10.1038/s41579-022-00820-y.
9. Q. Haq., M. Siddiqui, I. Sultan, A. Jan, A. Mondal, S. Rahman, Antibiotics, Resistome and Resistance Mechanisms: A Bacterial Perspective, Front Microbiol 9 (2018). https://doi.org/10.3389/fmicb.2018.02066.
10. J. Munita, C. Arias, Mechanisms of Antibiotic Resistance, Microbiol Spectr 4 (2016). https://doi.org/10.1128/microbiolspec.vmbf-0016-2015.
11. M. Chitsaz, M. Brown, The role played by drug efflux pumps in bacterial multidrug resistance., Essays Biochem 61 1 (2017) 127–139. https://doi.org/10.1042/EBC20160064.
12. H. Gao, L. Huang, C. Xu, X. Wang, L. Huang, G. Cheng, H. Hao, M. Dai, C. Wu, Bacterial Multidrug Efflux Pumps at the Frontline of Antimicrobial Resistance: An Overview, Antibiotics 11 (2022). https://doi.org/10.3390/antibiotics11040520.

13. A. Lorusso, J.A. Carrara, C.D.N. Barroso, F. Tuon, H. Faoro, Role of Efflux Pumps on Antimicrobial Resistance in Pseudomonas aeruginosa, Int J Mol Sci 23 (2022). https://doi.org/10.3390/ijms232415779.
14. K. Nishino, S. Yamasaki, R. Nakashima, M. Zwama, M. Hayashi-Nishino, Function and Inhibitory Mechanisms of Multidrug Efflux Pumps, Front Microbiol 12 (2021). https://doi.org/10.3389/fmicb.2021.737288.
15. A.A. Neyfakh, C.M. Borsch, G.W. Kaatz2, Fluoroquinolone Resistance Protein NorA of *Staphylococcus aureus* Is a Multidrug Efflux Transporter, 1993.
16. S. Santos Costa, M. Viveiros, L. Amaral, I. Couto, Send Orders of Reprints at reprints@benthamscience.net The Open Microbiology Journal, 2013.
17. Q.C. Truong-Bolduc, P.M. Dunman, J. Strahilevitz, S.J. Projan, D.C. Hooper, MgrA Is a Multiple Regulator of Two New Efflux Pumps in *Staphylococcus aureus*, J Bacteriol 187 (2005) 2395–2405. https://doi.org/10.1128/jb.187.7.2395-2405.2005.
18. T.S. Freitas, J.C. Xavier, R.L.S. Pereira, J.E. Rocha, F.F. Campina, J.B. de Araújo Neto, M.M.C. Silva, C.R.S. Barbosa, E.S. Marinho, C.E.S. Nogueira, H.S. dos Santos, H.D.M. Coutinho, A.M.R. Teixeira, In vitro and in silico studies of chalcones derived from natural acetophenone inhibitors of NorA and MepA multidrug efflux pumps in *Staphylococcus aureus*, Microb Pathog 161 (2021). https://doi.org/10.1016/j.micpath.2021.105286.
19. H.P. Goh, S. Dhaliwal, V. Kotra, Md.S. Hossain, N. Kifli, J. Dhaliwal, M.J. Loy, L. Ming, A. Hermansyah, H. Yassin, S. Moshawih, K. Goh, Pharmacotherapeutics Applications and Chemistry of Chalcone Derivatives, Molecules 27 (2022). https://doi.org/10.3390/molecules27207062.
20. J.E. Rocha, T.S. de Freitas, J. da Cunha Xavier, R.L.S. Pereira, F.N.P. Junior, C.E.S. Nogueira, M.M. Marinho, P.N. Bandeira, M.R. de Oliveira, E.S. Marinho, A.M.R. Teixeira Marinho, H.S. dos Santos Marinho, H.D.M. Coutinho, Antibacterial and antibiotic modifying activity, ADMET study and molecular docking of synthetic chalcone (E)-1-(2-hydroxyphenyl)-3-(2,4-dimethoxy-3-methylphenyl)prop-2-en-1-one in strains of *Staphylococcus aureus* carrying NorA and MepA efflux pumps, Biomedicine and Pharmacotherapy 140 (2021). https://doi.org/10.1016/j.biopha.2021.111768.
21. A.T.L. dos Santos, J.B. de Araújo-Neto, M.M. Costa da Silva, M.E. Paulino da Silva, J.N.P. Carneiro, V.J.A. Fonseca, H.D.M. Coutinho, P.N. Bandeira, H.S. dos Santos, F.R. da Silva Mendes, D.L. Sales, M.F.B. Morais-Braga, Synthesis of chalcones and their antimicrobial and drug potentiating activities, Microb Pathog 180 (2023). https://doi.org/10.1016/j.micpath.2023.106129.
22. Z.-Q. Yang, Y.-G. Hua, W. Chu, S. Qin, E. Zhang, Q.-Q. Yang, P. Bai, Y. Yang, D.-Y. Cui, Synthesis and antibacterial evaluation of novel cationic chalcone derivatives possessing broad spectrum antibacterial activity., Eur J Med Chem 143 (2018) 905–921. https://doi.org/10.1016/j.ejmech.2017.12.009.
23. H.H. Fokoue, P.S.M. Pinheiro, C.A.M. Fraga, C.M.R. Sant'Anna, Is there anything new about the molecular recognition applied to medicinal chemistry?, Quim Nova 43 (2020) 78–89. https://doi.org/10.21577/0100-4042.20170474.
24. D.N. Brawley, D.B. Sauer, J. Li, X. Zheng, A. Koide, G.S. Jedhe, T. Suwatthee, J. Song, Z. Liu, P.S. Arora, S. Koide, V.J. Torres, D.N. Wang, N.J. Traaseth, Structural basis for inhibition of the drug efflux pump NorA from *Staphylococcus aureus*, Nat Chem Biol 18 (2022) 706–712. https://doi.org/10.1038/s41589-022-00994-9.
25. D. Yusuf, A.M. Davis, G.J. Kleywegt, S. Schmitt, An alternative method for the evaluation of docking performance: RSR vs RMSD, J Chem Inf Model 48 (2008) 1411–1422. https://doi.org/10.1021/ci800084x.
26. A. Imberty, K.D. Hardman, J.P. Carver, S. Perez, Molecular modelling of protein-carbohydrate interactions. Docking of monosaccharides in the binding site of concanavalin A, Glycobiology 1 (1991) 631–642. https://doi.org/10.1093/glycob/1.6.631.
27. T.W. Johnson, K.R. Dress, M. Edwards, Using the Golden Triangle to optimize clearance and oral absorption, Bioorg Med Chem Lett 19 (2009). https://doi.org/10.1016/j.bmcl.2009.08.045.
28. P. Ertl, Polar Surface Area, in: Molecular Drug Properties, 2007: pp. 111–126. https://doi.org/https://doi.org/10.1002/9783527621286.ch5.
29. T.T. Wager, X. Hou, P.R. Verhoest, A. Villalobos, Central Nervous System Multiparameter Optimization Desirability: Application in Drug Discovery, ACS Chem Neurosci 7 (2016). https://doi.org/10.1021/acschemneuro.6b00029.

 doi:10.20944/preprints202509.2110.v1




30. X.L. Ma, C. Chen, J. Yang, Predictive model of blood-brain barrier penetration of organic compounds, Acta Pharmacol Sin 26 (2005) 500–512. https://doi.org/10.1111/j.1745-7254.2005.00068.x.
31. D. de Menezes Dantas, N.S. Macêdo, Z. de Sousa Silveira, C.R. dos Santos Barbosa, D.F. Muniz, A.H. Bezerra, J.T. de Sousa, G.G. Alencar, C.D. de Morais Oliveira-Tintino, S.R. Tintino, M.N. da Rocha, E.S. Marinho, M.M. Marinho, H.S. dos Santos, H.D. Melo Coutinho, F.A.B. da Cunha, Naringenin as potentiator of norfloxacin efficacy through inhibition of the NorA efflux pump in *Staphylococcus aureus*, Microb Pathog 203 (2025) 107504. https://doi.org/10.1016/j.micpath.2025.107504.
32. D.E. V Pires, L.M. Kaminskas, D.B. Ascher, Prediction and optimization of pharmacokinetic and toxicity properties of the ligand, in: Methods in Molecular Biology, Springer New York, New York, NY, 2018: pp. 271–284.
33. H. van de Waterbeemd, E. Gifford, ADMET in silico modelling: Towards prediction paradise?, Nat Rev Drug Discov 2 (2003) 192–204. https://doi.org/10.1038/nrd1032.
34. M. Pettersson, X. Hou, M. Kuhn, T.T. Wager, G.W. Kauffman, P.R. Verhoest, Quantitative assessment of the impact of fluorine substitution on P-glycoprotein (P-gp) mediated efflux, permeability, lipophilicity, and metabolic stability, J. Med. Chem. 59 (2016) 5284–5296.
35. E. V Radchenko, A.S. Dyabina, V.A. Palyulin, N.S. Zefirov, Prediction of human intestinal absorption of drug compounds, 2016.
36. A.S. Dyabina, E. V. Radchenko, V.A. Palyulin, N.S. Zefirov, Prediction of blood-brain barrier permeability of organic compounds, Dokl Biochem Biophys 470 (2016) 371–374. https://doi.org/10.1134/S1607672916050173.
37. E. V. Radchenko, Y.A. Rulev, A.Y. Safanyaev, V.A. Palyulin, N.S. Zefirov, Computer-aided estimation of the hERG-mediated cardiotoxicity risk of potential drug components, Dokl Biochem Biophys 473 (2017). https://doi.org/10.1134/S1607672917020107.
38. N. Le Dang, T.B. Hughes, G.P. Miller, S.J. Swamidass, Computationally Assessing the Bioactivation of Drugs by N-Dealkylation, Chem Res Toxicol 31 (2018) 68–80. https://doi.org/10.1021/acs.chemrestox.7b00191.
39. M. Zheng, X. Luo, Q. Shen, Y. Wang, Y. Du, W. Zhu, H. Jiang, Site of metabolism prediction for six biotransformations mediated by cytochromes P450, Bioinformatics 25 (2009). https://doi.org/10.1093/bioinformatics/btp140.
40. L. Di, C. Keefer, D.O. Scott, T.J. Strelevitz, G. Chang, Y.-A. Bi, Y. Lai, J. Duckworth, K. Fenner, M.D. Troutman, R.S. Obach, Mechanistic insights from comparing intrinsic clearance values between human liver microsomes and hepatocytes to guide drug design, Eur. J. Med. Chem. 57 (2012) 441–448.
41. R. Gonella Diaza, S. Manganelli, A. Esposito, A. Roncaglioni, A. Manganaro, E. Benfenati, Comparison ofin silicotools for evaluating rat oral acute toxicity, SAR QSAR Environ. Res. 26 (2015) 1–27.
42. Y. Wang, H. Venter, S. Ma, Efflux Pump Inhibitors: A Novel Approach to Combat Efflux-Mediated Drug Resistance in Bacteria., Curr Drug Targets 17 (2016) 702–719. https://doi.org/10.2174/1389450116666151001103948.
43. C. González-Bello, Antibiotic adjuvants – A strategy to unlock bacterial resistance to antibiotics, Bioorg Med Chem Lett 27 (2017) 4221–4228. https://doi.org/10.1016/j.bmcl.2017.08.027.
44. H.W. Boucher, G.H. Talbot, D.K. Benjamin, J. Bradley, R.J. Guidos, R.N. Jones, B.E. Murray, R.A. Bonomo, D. Gilbert, 10 × '20 progress - Development of new drugs active against gram-negative bacilli: An update from the infectious diseases society of America, Clinical Infectious Diseases 56 (2013) 1685–1694. https://doi.org/10.1093/cid/cit152.
45. J. Davies, G.B. Spiegelman, G. Yim, The world of subinhibitory antibiotic concentrations, Curr Opin Microbiol 9 (2006) 445–453. https://doi.org/https://doi.org/10.1016/j.mib.2006.08.006.
46. S. Zimmermann, M. Klinger-Strobel, J.A. Bohnert, S. Wendler, J. Rödel, M.W. Pletz, B. Löffler, L. Tuchscherr, Clinically Approved Drugs Inhibit the *Staphylococcus aureus* Multidrug NorA Efflux Pump and Reduce Biofilm Formation, Front Microbiol 10 (2019). https://doi.org/10.3389/fmicb.2019.02762.
47. G.W. Kaatz, S.M. Seo, Inducible NorA-Mediated Multidrug Resistance in *Staphylococcus aureus*, 1995.
48. G.W. Kaatz, S.M. Seo, Mechanisms of Fluoroquinolone Resistance in Genetically Related Strains of *Staphylococcus aureus*, 1997.

 doi:10.20944/preprints202509.2110.v1




49. L.M. Rezende-Júnior, L.M. de S. Andrade, A.L.A.B. Leal, A.B. de S. Mesquita, A.L.P. de A. Dos Santos, J. de S.L. Neto, J.P. Siqueira-Júnior, C.E.S. Nogueira, G.W. Kaatz, H.D.M. Coutinho, N. Martins, C.Q. da Rocha, H.M. Barreto, Chalcones isolated from Arrabidaea brachypoda flowers as inhibitors of nora and mepa multidrug efflux pumps of *Staphylococcus aureus*, Antibiotics 9 (2020) 1–12. https://doi.org/10.3390/antibiotics9060351.
50. M.M.R. Siqueira, P. de T.C. Freire, B.G. Cruz, T.S. de Freitas, P.N. Bandeira, H. Silva dos Santos, C.E.S. Nogueira, A.M.R. Teixeira, R.L.S. Pereira, J. da C. Xavier, F.F. Campina, C.R. dos Santos Barbosa, J.B. de A. Neto, M.M.C. da Silva, J.P. Siqueira-Júnior, H. Douglas Melo Coutinho, Aminophenyl chalcones potentiating antibiotic activity and inhibiting bacterial efflux pump, European Journal of Pharmaceutical Sciences 158 (2021). https://doi.org/10.1016/j.ejps.2020.105695.
51. J. da C. Xavier, F.W.Q. de Almeida-Neto, J.E. Rocha, T.S. Freitas, P.R. Freitas, A.C.J. de Araújo, P.T. da Silva, C.E.S. Nogueira, P.N. Bandeira, M.M. Marinho, E.S. Marinho, N. Kumar, A.C.H. Barreto, H.D.M. Coutinho, M.S.S. Julião, H.S. dos Santos, A.M.R. Teixeira, Spectroscopic analysis by NMR, FT-Raman, ATR-FTIR, and UV-Vis, evaluation of antimicrobial activity, and in silico studies of chalcones derived from 2-hydroxyacetophenone, J Mol Struct 1241 (2021) 130647. https://doi.org/10.1016/j.molstruc.2021.130647.
52. L. da Silva, I.A. Donato, S.R. Bezerra, H.S. dos Santos, P.N. Bandeira, M.T.R. do Nascimento, J.M. Guedes, P.R. Freitas, A.C.J. de Araújo, T.S. de Freitas, H.D.M. Coutinho, Y.M.L.S. de Matos, L.C.C. de Oliveira, F.A.B. da Cunha, Synthesis, spectroscopic characterization, and antibacterial activity of chalcone (2E)-1-(3′-aminophenyl)-3-(4-dimethylaminophenyl)-prop-2-en-1-one against multiresistant *Staphylococcus aureus* carrier of efflux pump mechanisms and β-lactamase, Fundam Clin Pharmacol 38 (2024) 60–71. https://doi.org/10.1111/fcp.12938.
53. L. da Silva, C.A.C. Gonçalves, A.H. Bezerra, C.R. dos Santos Barbosa, J.E. Rocha, Y.M.L.S. de Matos, L.C.C. de Oliveira, H.S. dos Santos, H.D.M. Coutinho, F.A.B. da Cunha, Molecular docking and antibacterial and antibiotic-modifying activities of synthetic chalcone (2E)-1-(3′-aminophenyl)-3-(4-dimethylaminophenyl)-prop-2-en-1-one in a MepA efflux pump-expressing *Staphylococcus aureus* strain, Folia Microbiol (Praha) (2024). https://doi.org/10.1007/s12223-024-01221-9.
54. L. Paixão, L. Rodrigues, I. Couto, M. Martins, P. Fernandes, C.C.C.R. de Carvalho, G.A. Monteiro, F. Sansonetty, L. Amaral, M. Viveiros, Fluorometric determination of ethidium bromide efflux kinetics in Escherichia coli, J Biol Eng 3 (2009) 1–13. https://doi.org/10.1186/1754-1611-3-18.
55. X.Z. Li, H. Nikaido, Efflux-mediated drug resistance in bacteria: An update, Drugs 69 (2009) 1555–1623. https://doi.org/10.2165/11317030-000000000-00000.
56. P. Ughachukwu, P. Unekwe, Efflux pump-mediated resistance in chemotherapy, Ann Med Health Sci Res 2 (2012) 191. https://doi.org/10.4103/2141-9248.105671.
57. S.R. Tintino, V.C.A. de Souza, J.M.A. da Silva, C.D. de M. Oliveira-Tintino, P.S. Pereira, T.C. Leal-Balbino, A. Pereira-Neves, J.P. Siqueira-Junior, J.G.M. da Costa, F.F.G. Rodrigues, I.R.A. Menezes, G.C.A. da Hora, M.C.P. Lima, H.D.M. Coutinho, V.Q. Balbino, Effect of vitamin K3 inhibiting the function of nora efflux pump and its gene expression on *Staphylococcus aureus*, Membranes (Basel) 10 (2020) 1–18. https://doi.org/10.3390/membranes10060130.
58. M.M. Marinho, M.N. da Rocha, E.P. Magalhães, L.R. Ribeiro, C.H.A. Roberto, F.W. de Queiroz Almeida-Neto, M.L. Monteiro, J.V.S. Nunes, R.R.P.P.B. de Menezes, E.S. Marinho, P. de Lima Neto, A.M.C. Martins, H.S. dos Santos, Insights of potential trypanocidal effect of the synthetic derivative (2E)-1-(4-aminophenyl)-3-(2,4-dichlorophenyl)prop-2-en-1-one: in vitro assay, MEV analysis, quantum study, molecular docking, molecular dynamics, MPO analysis, and predictive ADMET, Naunyn Schmiedebergs Arch Pharmacol 397 (2024) 7797–7818. https://doi.org/10.1007/s00210-024-03138-z.
59. G.R. Bickerton, G. V. Paolini, J. Besnard, S. Muresan, A.L. Hopkins, Quantifying the chemical beauty of drugs, Nat Chem 4 (2012) 90–98. https://doi.org/10.1038/nchem.1243.
60. C.A. Lipinski, Lead- and drug-like compounds: The rule-of-five revolution, Drug Discov Today Technol 1 (2004) 337–341. https://doi.org/10.1016/j.ddtec.2004.11.007.
61. J.D. Hughes, J. Blagg, D.A. Price, S. Bailey, G.A. DeCrescenzo, R. V. Devraj, E. Ellsworth, Y.M. Fobian, M.E. Gibbs, R.W. Gilles, N. Greene, E. Huang, T. Krieger-Burke, J. Loesel, T. Wager, L. Whiteley, Y. Zhang,

 doi:10.20944/preprints202509.2110.v1



Physiochemical drug properties associated with in vivo toxicological outcomes, Bioorg Med Chem Lett 18 (2008) 4872–4875. https://doi.org/10.1016/j.bmcl.2008.07.071.

62. C.D. de M. Oliveira-Tintino, J.E.G. Santana, G.G. Alencar, G.M. Siqueira, S.A. Gonçalves, S.R. Tintino, I.R.A. de Menezes, J.P.V. Rodrigues, V.B.P. Gonçalves, R. Nicolete, J. Ribeiro-Filho, T.G. da Silva, H.D.M. Coutinho, Valencene, Nootkatone and Their Liposomal Nanoformulations as Potential Inhibitors of NorA, Tet(K), MsrA, and MepA Efflux Pumps in *Staphylococcus aureus* Strains, Pharmaceutics 15 (2023) 1–15. https://doi.org/10.3390/pharmaceutics15102400.
63. M. Elshikh, S. Ahmed, S. Funston, P. Dunlop, M. McGaw, R. Marchant, I.M. Banat, Resazurin-based 96-well plate microdilution method for the determination of minimum inhibitory concentration of biosurfactants, Biotechnol Lett 38 (2016). https://doi.org/10.1007/s10529-016-2079-2.
64. J.M. Andrews, Determination of minimum inhibitory concentrations, Journal of Antimicrobial Chemotherapy 48 (2001). https://doi.org/10.1093/jac/48.suppl_1.5.
65. H.L. Yuen, S.Y. Chan, Y.E. Ding, S. Lim, G.C. Tan, C.L. Kho, Development of a Novel Antibacterial Peptide, PAM-5, via Combination of Phage Display Selection and Computer-Assisted Modification, Biomolecules 13 (2023). https://doi.org/10.3390/biom13030466.